Ireland Response

We greatly appreciate the thoughtful comments from referee Trevor Ireland, an expert in geochemistry and mass spectrometry who has worked with capacitor-based ion detection systems on the SHRIMP ion microprobe. The review is reprinted below in its entirety in italics with author responses shown by indentation where appropriate.

Referees Comment on ATONA Charge mode system.
Trevor Ireland, RSES ANU.

This is a timely paper concerning the introduction of the ATONA charge mode collection system to an ISOTOPX NGX.

The challenge of getting the the capacitative feedback system to work has been ongoing for a number of years. Both Cary and Keithley electrometers have had the ability to measure charge accumulation, but getting it to work in a routine analytical setup has been somewhat difficult (see Esat 1995, and Ireland et al. 2014).

> We have added a discussion of this background work to our introduction.

The physics behind charge mode and the implications for data collection are interesting, but are not particularly well explained in this paper. Potentially this is because of the patent that is being sought for this system. In any case, the issues concerning the noise floor for a capacitive system effectively relate to a "read" noise in the capacitor system as opposed to the Johnson Noise in a resistive system. Hence, there is a constant noise component in the capacitative read system (see Ireland et al. 2014), and the longer you integrate the better the signal to noise. On the other hand, you continually integrate Johnson Noise and so the signal/noise does not improve as quickly for an increase in integration time. For comparison, we have set up our capacitative system for a 2 s integration and the noise is similar to the 10e-13 ohm resistor, pretty much similar to what is achieved here. The 2s integration is appropriate for an ion microprobe because of the continual change in analytical conditions. A longer integration time is fine for a noble gas instrument because the gas is effectively homogenised in the source and there are only longer term fractionation processes to deal with.

> We have attempted to further clarify the operation of the ATONA system in light of these comments, but within the restrictions imposed by Isotopx' trade secrets. The constant noise component highlighted here is one of the advantages of the ATONA compared to the conventional resistor amplifier. In ATONA signal-to-noise ratio increases much faster with an increase in the integration time compared to the resistive amplifier. As suggested here, even longer integration times will be beneficial for more stable systems such as TIMS and stable isotope gas source mass spectrometers.

The work in the Isotope NGX is based around noble gas analysis, and specifically Ar isotopes. On one hand, this is a good system to look at because there is a good dynamic range in the isotope ratios under consideration. It also has the benefit that the ion beam is only changing at a (slow) steady rate allowing a good description of the progression of the counting statistics. The data show that the system performs well at the level commensurate with the measured ratios. On the other hand, Ar isotopes are not typically measured to high precision (e.g. as might be achieved for TIMS or ICP-MS analysis, or even SIMS analysis). This makes it also more difficult to establish the linearity of the system as well.

This is correct, although the measurements of stable zero-beam noise levels we present are an indication of the performance limits of the ATONA in a mass spectrometer with a more stable ion beam such as a TIMS. We expect results from TIMS labs with ATONA amplifiers to be published soon.

It is evident that the noise floor is still an issue for the 36Ar measurements described here. So as the volume of Ar gas is reduced, the error magnification from measuring the 36Ar/40Ar and resulting corrections to 40Ar/39Ar are still going to be a limitation and will likely still need to be carried out on an electron multiplier.

We do agree that the noise floor of the ATONA is comparable to an analog electron multiplier, but is not competitive with an ion counting electron multiplier for very small signals.

The benefit of the capacitative system is that measurements can be carried out on more Faraday cups, and potentially without the need for an electron multiplier (ion counter). The noise floor we have achieved is better than 500 c/s which means that for most isotope ratio measurements Charge mode is adequate and very often superior to an electron multiplier. At the upper level of count rates, 250-1000 x 10e3 c/s, the charge mode seamlessly connects with 10e12 ohm resistor capability. At the lower end, we have measured isotope ratios down to 10,000 c/s, which is well removed from the gain drift and dead time issues of an electron multiplier. As such charge mode does provide that connection between electron multipliers and the traditional resistor feedback amplifiers. But as demonstrated in this paper, it is a complementary aspect of the measurement of isotope ratios in geochemistry.

References

T.M. Esat, Charge collection thermal ionization mass spectrometry of thorium. International Journal of Mass Spectrometry and Ion Processes 148 (1995) 159–170.

T.R. Ireland, N. Schram, P. Holden, P. Lanc, J. Ávila, R. Armstrong, Y. Amelin, A. Latimore, D. Corrigan, S. Clement, J.J. Foster, W. Compston, Charge-mode electrometer measurements of Sisotopic compositions on SHRIMP-SI. International Journal of Mass Spectrometry 359 (2014) 26– 37.

Wielandt Response

We greatly appreciate the thoughtful comments from referee Daniel Wielandt, an expert in noble gas mass spectrometry who has published high-precision noble gas isotope ratio analyses on similar mass spectrometers. The review is reprinted below in its entirety in italics with author responses shown by indentation where appropriate.

Interactive comment on "The Isotopx NGX and the ATONA Faraday Amplifiers" by Stephen E. Cox et al.

Daniel Wielandt (Referee) wielandt@bio.ku.dk

Received and published: 13 March 2020

General comments: This is a well-written article on an important novel amplifier technology called ATONA that provides an otherwise currently unavailable combination of low noise and high dynamic range for Faraday cup measurements of ion beams. The technology could significantly improve both current and future mass spectrometers, and is therefore of general interest to all mass spectrometry specialists. I however believe that its impact could be improved by including some additional information as mentioned below. Alternatively, the suggestions in general comments should be addressed in future publications.

The article focuses on comparing the ATONA to current 10E11, 10E12, 10E13 and a hypothetical 10E14 ohm amplifier, or rather their idealized Johnson-Nyquist noise characteristics, for the purpose of multicollector noble gas measurements. ATONA outperforms ideal i.e. model 10E13 ohm amplifiers with respect to signal-noise ratio for 10 second integrations which is (most likely) an appropriate integration time for many measurements, and approaches an ideal (and currently commercially unavailable) 10E14 ohm amplifier for a 100 second integration which is most likely to long to properly sample and back-project a noble gas ion beam evolution to T0. The high dynamic range and low noise-fast response is definitely an improvement as compared to traditional amplifiers. This versatility means that amplifiers do not need not be physically or electronically switched among Faraday cups for different applications, which is an additional advantage that complements their low-noise characteristics. An ATONA could also be useful for single detector instruments that still have merit due to the high sensitivities afforded by the small volumes of such instruments.

Although the comparison with traditional amplifiers at low signal intensities is appropriate, the paper could benefit from a more stringent comparison with ion counters where the noise characteristics at low signal intensities are dominated by Poisson i.e. counting noise of the individual ion arrivals. This noise is inherent to counting atoms or ions and cannot be avoided. An interesting question is therefore under which beam intensity x time i.e. accumulated charge conditions the "baseline" noise in an ATONA becomes comparable to this inherent and unavoidable counting noise that will also be present and superimposed on zero-beam i.e. electronic baseline noise? This would seems to be an appropriate lower dynamic range where ion counters would (decisively?) outperform ATONA in terms of precision (but not necessarily accuracy). This number could presumably be calculated based on the 1-10-100 second zero-beam measurements that have already been carried out. It may also be possible to tease out that information from e.g. figure 7, but it is better that it is presented.

> It is true that the ATONA cannot replace ion counters for measuring very small signals. The baseline noise of the ATONA, while greatly reduced compared to other Faraday

amplifiers, is still larger than the near-counting-statistics noise level of an ion-counting multiplier. We show this, for example, in Figure 7, and we have added new discussion to the introduction clarifying the circumstances under which an ion-counting multiplier remains preferable. We also discuss in Section 3.2 that the ion counter remains necessary for very small signals on the NGX. We have also added a shot noise calculation to Figure 7.

The paper would also benefit if the working principles of ATONA were more thoroughly discussed (without disclosing confidential information). The patent documents contain a lot of public information that could be condensed into a description of the technology. I think the mass spectrometry community would be more likely to adopt the technology if they could understand it better, rather than using it as a "black box" technology where one might run into an unpredictable problem. As a naive non-engineer I personally would like to know how leakage current is reduced. Is there a maximum charge than can be accumulated before "discharging" if that is even the appropriate term? Are there hysteresis effects in the capacitor that make it particularly hard to drive out or sense low buildups of charge that might adversely affect linearity at low signal intensities? Can charge buildup in the Faraday-amplifier system start to deflect incoming ions, changing the peak shape thereby affecting e.g. pseudo-resolving peak-shoulder measurements. Does the "firmware" make decisions on sampling rate or readout parameters, switching between different regimes that depend on beam intensities?

We have endeavored to address these issues in the manuscript, and we address the specific points raised here in more detail in the response below.

Regarding leakage current: We assume that the reviewer is referring to the leakage current through the capacitor when there is non-zero charge accumulated. This leakage current is caused by migration of electric charges through the volume of the dielectric when an electric field is applied and creates non-linearity in measuring the accumulated charge over time, as part of the charge is lost through leakage during the measurement. Isotopx addressed this by first, the use of proprietary extremely low leakage dielectric for the feedback capacitor, then cooling the amplifier to reduce the already very small leakage current and then measuring its parameters to further compensate for the leakage. As a result, this error current is less than 1aA (10^{-18}A) for input currents above 1pA (10^{-12}A) creating <1ppm non-linearity. For smaller input currents the error current is reduces proportionally, 10^{-19}A for 100fA (10^{-13}A), 10^{-20}A for 10fA (10^{-14}A) and so forth, still maintaining <1ppm non-linearity. We have added this information to the manuscript.

Maximum charge: There is a maximum charge that can be accumulated by the feedback capacitor, which is determined by the value of the capacitor and the working voltage of the amplifier. However, the ATONA simply discharged the capacitor when it reaches the maximum value, a scenario that does not affect the measurement process. Only the rate of change of the transimpedance amplifier output voltage and therefore the rate of change of the accumulated charge is measured. This rate of change does not depend on the maximum charge value and the maximum value of the measured current depends only on the dynamic properties of the amplifier and subsequent data acquisition circuitry.

Hysteresis: Dielectric hysteresis may be defined as an effect in a dielectric material similar to the hysteresis found in a magnetic material. This causes a static shift in the

capacitor voltage for a certain charge dependent on the history of previous charges/discharges. Isotopx addressed this by the use of proprietary dielectric with paraelectric properties and with negligible hysteresis. As a result, the effect of capacitance-voltage hysteresis on output voltage is unobservable.

Charge buildup: The Faraday buckets are directly connected to the input of the inverting amplifier. This fixes the voltage of the bucket at zero volts all the time regardless of the accumulated charge and therefore does not create any change or deflection in the incoming ions beams. We have added this information to the manuscript.

Firmware/black box decisions: No. The firmware neither changes any acquisition parameters, e.g. sampling rates, voltage ranges, measurement regimes or any other parameter, nor switches/changes any hardware values or components for any reason. This is done to preserve continuity, linearity, and repeatability of the measurements throughout the entire dynamic range.

Throughout: The term Johnson-Nyquist noise is used in line 114, but then subsequent usage is about Johnson noise. Should abbreviate it JN-noise at first usage, and then refer to it as such subsequently.

We have adjusted the text as suggested for better clarity.

When discussing the performance using air and cocktail standards, it would be nice to have the approximate beam intensities tabulated in e.g. fA as that it the unit that is already reported for noise measurements.

We have added this information where appropriate.

Specific: First paragraph i.e. 8-22 could perhaps use a statement regarding engineering tradeoffs regarding multicollection versus volume/sensitivity, i.e. the increase in volume that tends to occur with multicollection and the related drop in sensitivity. This is one reason why single collector instruments still have a role. In fact, the versatility of the ATONA seems to make it very well suited for that role; this is only aided by its rapid response as discussed later.

We agree with both the principle of the statement regarding the value of small volume instruments and with the possible role of the ATONA in such instruments, both because of its dynamic range and because of its response time. We have added statements to this effect to the second paragraph of the manuscript.

Second paragraph, line 30. Mention of long settling time for high value resistors is relevant in case of dynamic measurements, but static multi-collection of noble gases all but removes the settling time issue since any single resistor only measures one very slowly evolving beam. This should be mentioned in order to be fair to the current generation of high-ohm multi-collector equipped instruments.

While it is true that settling time is less important for multicollector instruments, it can be long enough on some high-gain RTIAs that without mitigation it affects the settling time of the measurement on the time scale of gas inlet. We have added this caveat to the manuscript.

Paragraph 6, Line 80. Could the authors perhaps make a back of the envelope error propagation calculation of how much of the air correction error on a blank subtraction on their instrument would arise from the 36Ar using a ion counter versus the ATONA? Or conversely the calculations suggested in the general comments regarding comparison of counting noise vs zero beam noise? This would be highly relevant for e.g. Ar or Ne dating of young samples where samples or fractions may be comparable in intensity to blanks.

We have added such a calculation for a typical young basalt sample.

Paragraph 7, Line 84. If possible, it would be nice if the patent were hyperlinked.

We have provided a hyperlink.

Paragraph 9 A formulation of Johnson-Nyquist noise with some appropriate reference and description would be useful for non-specialists.

We have added additional information.

Paragraph 11, Lines 130-140. This is a bit hard to read, and the reporting would benefit from a data-table showing the noise characteristics for 1, 10 and 100 second integrations with ATONA and 10E11-14 resistors. In such a way, one could focus on describing the noise "crossover" points for the various detector technologies that most readers would be searching for anyway as seen in figure 4.

We have added the requested table as Table 1.

Figure 6 (and figure A1) It is hard to identify the ranges, could the color code somehow be complemented by a change in marker style? It might also be a good idea to write the ranges as from 200% to 0.36% rather than between 200% and 0.36%.

In response to this comment and a comment from Kuiper, we have reorganized the figures so that the analyses are grouped by signal size rather than by analysis order, which we hope will also address the difficulty in distinguishing them from one another. The point about the ranges being inclusive is noted and this change has also been made.

Figure 7 We should expect a number of inflection points where all faraday mass spectrometer technologies gradually switch to follow a slope determined by counting noise (N^0.5) rather than signal over "baseline" JN or kTC noise (N^1). The linear error envelopes could give the erroneous impression that Faraday-based technologies can eventually outperform counting noise at high intensities, this should be avoided.

We have added a line showing the calculated uncertainty limit for a time-zero regression through data affected only by shot noise.

Table 1 The table should include the intensity of the smallest ion beam intensity i.e. the 36Ar intensity in fA. It would also be nice to have (and discuss) an MSWD to compare internal

precision and external reproducibility for all the measurements. A calculated average for the different intensities would also be nice, and could be plotted to evaluate non-linearity.

> The uncertainties shown at the bottom of the table are in fact the population uncertainties. We have added a line also showing the averages as requested, which should also make it more clear that what is meant by the 1-sigma uncertainties at the bottom (this is also in response to a comment by Kuiper). The averages are all well within uncertainty of one another, but an experiment aimed at properly assessing isotope ratio linearity would require many more measurements for the smaller signal sizes.

Table A1 The table should include the intensity of the smallest ion beam intensity i.e. the 38Ar intensity in fA. It would also be nice to have (and discuss) an MSWD to compare internal precision and external reproducibility for all the measurements. A calculated average for the different intensities would also be nice, and could be plotted to evaluate non-linearity.

Data for 0.36% measurements seem improbably precise, are they missing a digit

> See notes from above. And yes, thank you for catching that—the table was hanging off the edge of the page, truncating the internal uncertainties for these measurements. The tables have been modified to fit the page better.

It would also be nice to discuss the presumably significant decrease in precision when going from 5.2% aliquots to 2.6% aliquots and lower. Is this a characteristic of ATONA, or is it due to error propagation effects from subtraction of blank 38Ar + H37Cl?

> While the uncertainties increase for smaller signal sizes, the relationship is as expected and is primarily governed by the measurement uncertainty of the smaller ion beam. We discuss this further in Section 3.2 and show it in Figure 7.

Kuiper Response

We greatly appreciate the thoughtful discussion comments from Klaudia Kuiper, an expert on Ar geochronology who has worked extensively on questions of precision and statistics in the field. The review is reprinted in its entirety in italics with author responses shown by indentation where appropriate. Some comments were also addressed in the response to the Wielandt review.

Interactive comment on "The Isotopx NGX and the ATONA Faraday Amplifiers" by Stephen E. Cox et al.

Klaudia Kuiper k.f.kuiper@vu.nl

Received and published: 13 March 2020

General comments This article describes the performance of a new patented type of capacitive transimpendence amplifier (CTIA) for noble gas mass spectrometry. Due to trade secrets the exact working of this amplifier is not described, only its performance is tested and compared to other commonly used amplifier technology. This seems to be a new step in amplifier development and although not fully disclosed, this is an development that likely will be implemented by several labs in the next 5 years or so. I therefore consider this paper worth publishing, because it is relevant for the community to judge the possible advantages and disadvantages of this new CTIA. The papers is well written clearly describes the experiments and tests that have been performed.

Specific comments and technical issues

Line 38 "as those are that are" → remove "are"

> We have corrected this typo.

Line 63 "through small leaks". What do you consider small leaks?

> We have changed the word "small" to "undetectable" to clarify that we mean small inputs of gas that are too small to be considered problematic and would not be detected through leak checking.

Line 77-80: What about 37 beam. This is also a very small beam on e.g. young sanidine grains (can now possible be addressed with ATONA).

> Sanidine will have very low 37Ar; the size of this beam will still be far too small to measure precisely with the ATONA. This is especially true for young sanidine, which typically undergoes very short irradiation. The other side of this coin is that the correction is so small that the precision we obtain is acceptable. It is certainly true that we are measuring 37Ar more precisely on the NGX with ATONA than on previous instruments.

Line 96-97: Not fully clear, can you give examples of approaches you are thinking of (even tough not fully tested)?

We have added an example of a measurement approach that will be possible with the production version of the ATONA hardware (it is not possible with the protoype version we used here).

Line 130-131: Can you provide used equations and calculations in appendix?

We have added the equation to the appendix.

Line 142: modify to "approximately 8.5×10-13 moles of 40Ar per aliquot"

We have clarified that the amount of Ar is calculated per aliquot.

Line 146-149: Can you quantify? What signals did you expect based on your approximations and based on GLO? What is the 40Ar content in your GLO standard? And I'll assume you mean APIS with the manometrically calibrated volume. Can you add an estimate of your system's sensitivity?*

I think the original wording of this section makes it sound like something more complicated is happening here. The standard used in this paper was prepared without first doing a manometric volume calibration for the machined pipette, so the point of this section is just to say that the precise size of this particular standard is known from a comparison to properly volume-calibrated air standard in a different tank. APIS is not involved. The calculated sensitivity was also compared favorably to GLO in the course of normal analyses on several occasions, but this is not used as part of the primary calibration and is not particularly important, so I have removed this remark for clarity. Hopefully the changes in the manuscript make all of this more clear. The sensitivity of the mass spectrometer is described elsewhere in the paper.

Line 152: Can you add for clarity 100% (8.5×10-13 moles 40Ar), 37.7 % (x moles 40Ar) etc

Yes, we have added this information.

Line 211: "our lab standard" which is?

The original wording in the paper is very confusing. The lab standard is the afore-mentioned air standard. The other air standard is the air standard that is part of the APIS. We have clarified this in the manuscript.

Line 213-214: "so a direct comparison of measured ratios is not possible" Comparison with what?

We have added "between labs." The original purpose of the APIS experiment was to allow mass spectrometers to be compared after measuring exactly the same gas. While the comparison is still useful, the noticeable amount of air contamination over time requires that the ratios first be corrected before comparison.

Line 224-225: "gain bias of the amplifiers is significantly more stable than both RTIAs and electron multipliers" This paper does not really provide data for comparison of gains for RTIAs and ATONA. Only gain data of ATONA are shown.

This is a fair point. We have changed this to focus on noise levels and to clarify the comparison to the ion-counting multiplier. The preliminary data we cite from TIMS instruments (Szymanowski and Schoene, 2019) will show more clearly that the gain stability of the ATONA is superior to existing RTIAs. In our case, we do not have an independent electronic calibration on the prototype unit, and the stability of the signal is limited by the noble gas mass spectrometer ion source rather than by drift in the amplifiers.

Figure 1: add the unit between brackets to the Y-axis title (e.g. cps). In caption it is mentioned that Faraday data are reported in Volts, in line 110-111 it is stated that you convert back to beam current for easier comparison.

This figure shows the output as displayed in the current version of the pychron software, which is not how we present the data elsewhere in the paper. For this reason, we clarify the display units in the caption.

Figure 3 and text line 112-115: can you add your calculations / formulas used for RTIA noise to the appendix. Inset is really small and hard to read (especially when printed)

The formula has been added to the appendix. I am also adding the full version of the inset figure to the appendix because I do not think it merits another figure in the paper and the template restricts the size of the figures, so it is difficult to make the inset more readable.

Figure 5: Is 40Ar/38Ar the t0 intensity of 40Ar air minus t0 intensity of 40Ar blank divided by the t0 intensity of 38Ar air minus t0 intensity of 38Ar blanks? How many blanks are run? In the legend there are only circle symbols, in the figure also squares. The way data are plotted suggests that Xact and ATONA measurements are bracketed. Can you first plot the Xact 100% data, followed by ATONA 100% data etc.?

We have expanded the description of the measurement scheme in the caption and changed the figure as suggested. Thank you for catching the error in the legend.

Figure 6. Maybe a matter of reader preference, but I prefer to see the 10 different analyses of one beam size plotted combined instead of interspersed. Now I find it difficult to see that variation within 10 similar experiments. And we are looking at ratios of blank corrected time zero intensities of 40 and 36? Inset is again rather small.

The figures have been changed, and information requested added to the caption.

Figure 7. The ARGUS RTIA data are from NMGRL? And are the measured with m/e36 on a Faraday with RTIA or multiplier? Colors of shaded lines are similar, not clear what they are showing.

I added a reference to the paper section that describes the comparison datasets, which I think are too extensive to put in this already-lengthy caption. The shaded lines are an attempt to guide the eye to the many different groups of data points in the figure, and I have clarified this in the caption. I recognize that this figure is busy and that they are

hard to distinguish, but I think making them bolder would obscure the more-important data points themselves.

Figure 8: in caption it is indicated that smaller aliquots are on the left, and larger on the right. Can you indicate different areas in the figure which are the 0.1cc, the 0.2cc aliquots etc. The NMGRL Argus measurements are with 40Ar on H2 with 10^12 Ohm amplifier and 36 on L2 with 10^13 Ohm amplifier? Do Argus data with 40Ar on H1 with 10^12 or 10^13 Ohm amplifier and 36Ar on L3 multiplier also exist? And if yes, how do they compare? Did NMGRL perform exactly the same experiment with 3 aliquots per pipette volume? And if not, what are the criteria to select these 3 data points?

The experimental protocol was (as close as possible) to identical during the APIS experiments, which hopefully will be published eventually. I have added this information to the caption. This represents the complete dataset. The requested clarification has been added to the figure.

Table 1: what is the ± in the header row? 1SD? What is the 1-σ at the bottom of the table: the standard deviation of the ten measurements? Can you also report the mean (or the weighted mean)?

I have clarified the latter points and added a note in the caption stating that uncertainties are 1-sigma standard deviation.

Figure A1: I don't like the interspersed way of plotting. Also with all the colors that look rather similar it is difficult to see what is what.

This has been changed.

Figure A2: what is exactly plotted on the Y axis? Why not signal divided by average AX signal? Then the intercalibration factors mentioned in caption are immediately clear. And what is plotted on the X-axis? Why are there no data of aliquots 817, 820 etc. What is the beam size used for this intercalibration, is a baseline correction needed? And I'll assume data are regressed to time zero using a linear fit? What is the settling time, maybe worth mentioning, because a similar approach using RTIAs will take longer

This is exactly what is being done, only then the data are shown using delta units because the ratios are so close to unity. This is unclear, so I have changed the figure to simply show the ratios. The aliquot numbers represent extraction numbers from the air pipette, and the missing aliquot numbers were standards that were measured in typical multicollection mode in between intercalibration measurements. This is not meaningful outside of the lab and has been removed. The beam size is the full air standard described elsewhere; this has been clarified, along with details of the measurement scheme.

The Isotopx NGX and the ATONA Faraday Amplifiers

Stephen E Cox[1], Sidney R Hemming[1, 2], and Damian Tootell[3]

[1]Lamont-Doherty Earth Observatory, the Earth Institute at Columbia University, 61 Route 9W, Palisades, NY 10964, USA
[2]Department of Earth and Environmental Sciences, Columbia University, New York, NY 10027, USA
[3]Isotopx, Ltd., Dalton House, Dalton Way, Middlewich CW10 0HU, UK

Correspondence: Stephen E Cox (stephen@stephencoxgeology.com))

Abstract. We installed the new Isotopx ATONA Faraday cup detector amplifiers on an Isotopx NGX mass spectrometer at Lamont-Doherty Earth Observatory in early 2018. The ATONA is a capacitive transimpedance amplifier, which differs from the traditional resistive transimpedance amplifier used on most Faraday detectors for mass spectrometry. Instead of a high gain resistor, a capacitor is used to accumulate and measure charge. The advantages of this architecture are a very low noise floor, rapid response time, stable baselines, and very high dynamic range. We show baseline noise measurements and measurements of argon from air and cocktail gas standards to demonstrate the capabilities of these amplifiers. The ATONA exhibits a noise floor better than a traditional 10^{13} Ω amplifier in normal noble gas mass spectrometer usage, superior gain and baseline stability, and an unrivaled dynamic range that makes it practical to measure beams ranging in size from below 10^{-16} A to above 10^{-9} A using a single amplifier.

1 Introduction

The design of analog ion collectors for mass spectrometry has changed strikingly little for seventy years. Early instruments already employed much of the detector technology we recognize today, including multiple collectors, secondary electron suppressors, and electronic circuits that employed high-value resistors (resistor transimpedance amplifiers, or RTIA) to amplify small currents to measurable voltages (e.g., Nier, 1940, 1947). Between the 1950s and 1980s, as the field of isotope geochemistry shifted from home-brewed instruments to commercial ones, available noble gas mass spectrometers consolidated around a design based on the Reynolds mass spectrometer using a "Nier-type" ion source, a fixed accelerating voltage, a variable magnetic field, and a single pair of collectors consisting of an analog electron multiplier (later an ion counting multiplier) and a Faraday cup, intended to be used separately for signals of different sizes (e.g., Reynolds, 1956; Bayer et al., 1989; Renne et al., 1998; Burnard and Farley, 2000). Since around 2010, multicollection has come back into vogue as improvements in electronic noise and stability have mitigated the problems of comparing beams measured on two separate amplifiers, and the field has sought ways to minimize the uncertainty conferred by the fitting of gas evolution trends in order to calculate isotopes ratios at the time of sample inlet (e.g., Mark et al., 2009; Coble et al., 2011).

The shift toward multicollection has been accompanied by a diversification of the collector technologies available, with new ion counting multipliers built with a geometry that allows multicollector spacing, and new RTIA Faraday amplifiers employ-

ing higher-value resistors in order to take advantage of the $\sqrt{R}$ relationship between normalized signal noise and resistance (e.g., Zhang et al., 2016). These advances are not without trade-offs, however. ~~The use of~~ For one, multicollection requires the use of wider flight tubes and larger collector blocks that increase the volume of static vacuum instruments, reducing their effective sensitivity; some applications may still benefit from the use of small volume single collector instruments, for which fast, high-dynamic-range detectors are particularly valuable. One some multicollector instruments, the use of ion counting multipliers in the detector position for large beams (^{40}Ar, for example) ~~on some instruments allows them to measure~~ allows the measurement of very small samples but limits ~~their~~ the dynamic range (Jicha et al., 2016). Instruments using high-value resistor amplifiers to achieve the same goal also suffer from a loss of dynamic range, although it is not as severe, but additionally suffer from long settling times (large Tau; this problem is less severe on multicollectors that do not need to peak hop, but can still affect signal stability during the start of a measurement), baseline instability, and drift in gain calibration. Indeed, these problems have limited the use of such collectors for decades, but the cost-benefit calculation has shifted due to improving electronic stability and new techniques for dealing with the Tau-correction (Zhang et al., 2016), as well as a cultural shift in the priorities of noble gas geochemistry labs toward young, small samples and higher precision (e.g., Wijbrans et al., 2011; Jicha et al., 2012; Mark et al., 2017; Rose and Koppers, 2019).

However, the desire to measure young samples well has not displaced the need to measure old samples very precisely (Sprain et al., 2015), to measure large amounts of noble gas in ice core and water samples (Lu et al., 2014), and to measure extreme abundance ratios such as those ~~are~~ that are typical in ^{3}He/^{4}He analyses (Espanon et al., 2014). The ideal collector, therefore, has not just a low noise floor and high sensitivity, but also a high dynamic range, the ability to switch between low and high signals with no memory, and a stable, precisely measurable gain bias between each detector. Resistor Faraday amplifiers have a fairly restricted dynamic range, with the ability to reliably measure signals over only about five orders of magnitude. Ion counting multipliers are only able to measure small signals, and suffer from significant nonlinearity at the upper and lower ends of their useful range. Analog multipliers have a much higher dynamic range, about eight orders of magnitude, but suffer from both nonlinearity and relatively short timescale gain drift. In addition, electron multipliers wear quickly and are both expensive and vulnerable to damage from vacuum accidents and large ion beams. Faraday cups are extremely linear, quiet, resilient, and cheap to manufacture, so a technological solution that extends their useful dynamic range and sensitivity to small signals is highly desirable.

Mass spectrometers have always relied on transimpedance amplifiers, which consist of an active circuit element (usually an op-amp) that converts a small input current to a high output voltage (Figure 1). The capacitive transimpedance amplifier was developed decades ago, and was an option on such venerable devices as the Keithley 6512 Electrometer, which provided the option of feedback resistors or capacitors for current measurements. The advantage of the latter was seen as the high dynamic range, while the disadvantages were the accuracy and linearity. More recent work has demonstrated the promise of low noise and stability using feedback capacitors, but with serious limitations on dynamic range, linearity, and flexibility caused by the measurement of accumulated charge and the need to handle routine discharging of the feedback capacitor

(Esat, 1995; Ireland et al., 2014). The new ATONA capacitive transimpedance amplifier developed by Isotopx maintains the high dynamic range (effectively unlimited for noble gas measurements) and rapid response time of the earlier feedback capacitor devices while also delivering the linearity and accuracy more traditionally associated with resistor transimpedance amplifiers. The ATONA uses a proprietary extremely low leakage dielectric for the feedback capacitor combined with a cooled amplifier housing to reduce the leakage current, and consequent nonlinearity, to below 1 ppm. Unlike previous charge-mode amplifiers, the ATONA measures rate of change of the transimpedance amplifier output voltage and therefore the rate of change of the accumulated charge. The advantages of this setup, which can accurately measure extremely low signals without sacrificing stability or the ability to measure large signals, are significant for noble gas mass spectrometry and for mass spectrometry in general.

Noble gas mass spectrometers must measure an evolving signal due to the action of the instrument itself on the sample (Figure 2). Sample abundances are typically so small that the entire sample is allowed to equilibrate with the vacuum inside the mass spectrometer at the beginning of analysis, which requires that the pumps be isolated from the vacuum chamber. Starting at this time, confounding gases will be introduced through ~~small~~ undetectable leaks and desorption from the walls of the vacuum chamber housing the mass spectrometer, and sample gas will be consumed by ionization in the ion source and implantation in either the collector or the walls of the vacuum chamber. Because these processes change the gas composition, and therefore both the abundances and the ratios of the noble gas isotopes being measured, noble gas geochemists typically extrapolate the evolving gas signal back to the time of sample inlet—commonly referred to as "time zero"—meaning that the analysis loses statistical power as it continues in time. The advent of multicollection means that isotope ratios could be computed directly at each time point and then themselves extrapolated to "time zero," but so far noble gas geochemists have largely used multicollection simply as a means to ensure that the maximum amount of data can be collected simultaneously for each isotope.

2 Isotopx NGX and ATONA amplifier

The Isotopx NGX is a multicollector noble gas mass spectrometer with a Nier-type ion source, a Hall Probe feedback-controlled electromagnet mass analyzer, and a customizable collector block comprising fixed Faraday cup and ion counting electron multiplier detectors. The source sensitivity is approximately 10^{-3} A/Torr, the ^{36}Ar background is approximately 2×10^{-19} moles, or 5×10^{-15} cc STP, and the rise is approximately 8×10^{-18} moles, or 2×10^{-13} cc STP ^{40}Ar per minute. The NGX at LDEO has five fixed detectors, four Faraday cups and one electron multiplier, in the appropriate configuration to simultaneously collect the five isotopes of argon typically measured for ^{40}Ar/^{39}Ar dating: ^{40}Ar, ^{39}Ar, ^{38}Ar, ^{37}Ar, and ^{36}Ar. The electron multiplier is placed at the ^{36}Ar position, where signals are typically relatively small and must be measured with high precision due to the need for an accurate ^{40}Ar/^{36}Ar ratio for initial Ar correction. We chose this configuration before the ATONA became available, and in fact we believe that an ATONA would be appropriate for ^{36}Ar measurement in many ~~(but not all) situations.~~ situations. An instrument with the ability to switch between measuring ^{36} Ar on an ATONA an an electron multiplier would be able to take advantage of the stability and dynamic range of the ATONA for large ^{36} Ar signals while still using an ion-counting electron

multiplier for very small signals. For example, a single heating step on a very young basalt sample may yield 10^{-14} moles of ^{40}Ar, of which 95% is non-radiogenic. In this case, the uncertainty of the ^{36}Ar measurement will dominate the trapped Ar correction to the ^{40}Ar and therefore the age uncertainty, and we would choose to measure the 3×10^{-17} mole ^{36}Ar signal with the ion counter with 0.2% uncertainty rather than using the ATONA with 3% uncertainty.

After initial installation in late 2017 with Isotopx 10^{11} Ω and 10^{12} Ω Xact amplifiers, we installed a prototype set of ATONA amplifiers on the NGX in March 2018. The ATONA is a capacitive transimpedance amplifier, which is partially described in ~~UK patent application GB2552232~~UK patent GB2552232. The remaining aspects of the amplifier are protected as trade secrets. The ATONA substitutes the typical high-gain resistor of an RTIA, for which one would try to minimize the capacitance of the circuit, with a capacitor and a series of proprietary circuits that allow the rate of charge accumulation (rather than the accumulated charge itself) to be continuously sampled (again, the exact mechanism used is a trade secret). ~~The~~ Because the ATONA relies on a measurement of the rate of charge accumulation, it simply discharges the feedback capacitor when the rated capacitance has been reached in a process that is transparent to the measurement itself. The proprietary paraelectric dieletric material minimizes nonlinearity due to current leakage and dielectric hysteresis. Because the Faraday buckets are directly connected to the input of the inverting amplifier, the voltage of the bucket is fixed at zero volts regardless of the accumulated charge on the capacitor and therefore charge buildup that might affect ion behavior is avoided. The result is that the ATONA can measure a wide range of ion beam currents, from attoamps to nanoamps (hence the name), with good linearity, very low noise, and a settling time short enough to be insignificant (less than the 2 ms sampling time of the measurement electronics).

The ATONA has the important characteristic that the noise scales inversely with time, rather than with the square root of time, so accumulating a signal for longer between sampling intervals will result in a linearly less noisy signal. Counting statistics reduces uncertainty with the square root of time, so by comparison the ATONA gains an additional factor of the square root of time in noise reduction when the sampling interval is extended. There is a trade-off in noble gas mass spectrometry because of the evolution of the signal with time, although it is important to mention that the signal from the production version of the ATONA can be subsampled without sacrificing the gain of the longer sampling time. This dynamic opens up a wide array of possibilities of best measurement practice that will vary with ion beam size, and we have not yet fully explored them; for example, one might choose a longer integration time for smaller beams that are measured as an average and a shorter integration time for larger beams during the same measurement. The work presented here has led us to settle on an integration time of 10 seconds, with a typical total analysis time of 600 seconds in multicollection mode, as a sweet spot for reducing noise without sacrificing gas evolution fit statistics. Analytical conditions for different experiments in this study vary and are described in the figure captions. All isotope evolutions are fit using a linear regression with no outlier data points excluded from either fits or uncertainty calculations, and with no measurement cycles discarded from the analysis. The only exception is in Section 3.3, in which we removed the final 200 seconds from a set of 600-second APIS analyses in order to allow a direct comparison to a dataset of 400-second analyses on a different mass spectrometer.

3 Analyses of electronics and gas standards

3.1 Background noise

Reported detector signal units are an arbitrary choice in mass spectrometry; the important quantity for a given detector is signal/noise ratio produced by a given incident ion beam. We quantify this by converting measured signal from detector units to incident ion beam current using Ohm's Law for voltage measured on an RTIA. The ATONA does not measure voltage in the same way as an RTIA, but its firmware converts the signal to equivalent 10^{11} Ω RTIA volts. We convert back to beam current for clearer comparison with RTIAs that have a different gain, and with other types of detectors. As an example, 1 10^{11} Ω RTIA volt is equivalent to 10^4 fA, and 625 cps on an ion counting electron multiplier is equivalent to 0.1 fA. We calculate background noise for ideal RTIAs with a variety of feedback resistors. In this case, we assume that the only significant component of noise is Johnson–Nyquist (J–N) noise, or thermal white noise, which is an inherent property of all conductors. The observed noise is caused by the the movement of charge within the conductor in response to random fluctuation caused by thermal radiation, as described by Nyquist (1928) (See Appendix A for equation). J–N noise provides an absolute limit for the signal/noise ratio achievable with an RTIA. ~~The~~ , and the best commercial RTIAs approach this limit.

Unlike ~~Johnson~~ J–N noise, kTC noise (capacitor thermal noise, equal to the product of the Boltzmann constant, k, and the absolute temperature, T, divided by the capacitance, C) has no frequency component. This means that the voltage noise produced by a current discharged from a capacitor will scale linearly with time. As a result, one might expect to achieve a factor of $1/\sqrt{t}$ in noise reduction by extending the charge accumulation time arbitrarily. This is not exactly how the ATONA functions, as one is able to subsample the measurement without losing the benefit of a longer integration time, but the expected linear relationship is achieved, similar to previous systems in which the charge of the capacitor is read directly (Ireland et al., 2014). The theoretical noise floor of the ATONA design is not immediately apparent from the publicly-available information about its capabilities, which do not reveal either the design of the measurement circuit or the value of the capacitor employed. A simple calculation assuming kTC noise is the only source of noise on each ATONA measurement yields a value of ~~15-20~~ 15–20 pF for the complete circuit, which includes both the capacitor used on the amplifier and the capacitance of the Faraday collectors themselves and the wires and feedthroughs that connect them. We measure noise directly through a series of measurements on the Isotopx NGX with the instrument under vacuum, all lenses active, and the filament powered off. We then express this noise floor in terms of incident ion beam for direct comparison to RTIAs.

The results are shown in Table 1 and are plotted in two different ways. First, we show a series of measurements of ATONA noise compared to ideal RTIA ~~Johnson~~ J–N noise calculations for a series of RTIA resistor values in Figure 3 (see Appendix A). This figure simply shows measurements taken with the ATONA with no ion beam, with the arithmetic mean of the measurements subtracted from each. This is, therefore, what a series of measurements of a stable beam would look like to the user during a measurement cycle. Each measurement is made with a ten second integration, which is the typical integration time we use for the ATONA on most samples. The ATONA measurements have a standard deviation of 0.0085 fA, which is equivalent

to 0.85 μV on a 10^{11} RTIA. In Figure 4, we show the same noise data as 1-σ standard deviation of a signal plotted as a function of integration time to show the different behavior of the ATONA as integration time is changed. Using a one second or 100 second integration time, the ATONA measurements have standard deviations of 0.073 fA and 0.0018 fA, respectively. The ten-second integration time value compares favorably to a 10^{13} RTIA at 0.011 fA, but does not quite reach the low noise level of a 10^{14} RTIA at 0.0040 fA. Similarly, at one second integration, the ATONA is in between the 10^{12} and 10^{13} RTIA (0.40 fA, 0.037 fA, respectively).

3.2 Air standards

We prepared a large air standard of approximately 8.5×10^{-13} moles of Ar per aliquot for mass spectrometer installation and initial testing. We used air taken at a distance from the Lamont-Doherty Earth Observatory Comer geochemistry building in Palisades, NY, on a dry day in November, and we filled the approximately six liter standard tank with one aliquot from the approximately 0.1 cc pipette. Subsequent aliquots for measurement were taken from the standard tank using the same pipette, attached to a custom-built high vacuum system containing a hot SAES St101 getter. ~~The~~ No primary volume calibration was performed on the pipette for the large standard, so the size of the ~~resulting Ar aliquot introduced to the mass spectrometer was estimated first~~ Ar aliquot was first roughly estimated from the approximate volumes of the standard tank, pipette, and vacuum system, then ~~refined by comparison to the GLO glauconite argon concentration standard and by comparison to a standard tank on another mass spectrometer with a manometrically calibrated~~ calculated using intercalibration with a second standard tank with a manometrically-calibrated pipette volume.

We measured four different splits of the air standard ranging from the full aliquot (8.5×10^{-13} moles ^{40}Ar) to approximately 0.36% of the total (3.1×10^{-15} moles ^{40}Ar). The split sizes of 100%, 17.7% (1.5×10^{-13} moles ^{40}Ar), and 2.6% (2.2×10^{-14} moles ^{40}Ar) are most useful for comparing the Isotopx Xact RTIA to the ATONA. For all Xact measurements, a 10^{11} Ω amplifier was used for ^{40}Ar and a 10^{12} Ω amplifier was used for ^{38}Ar. The ATONA amplifiers all use the same feedback capacitor and are therefore interchangeable. The ^{40}Ar/^{38}Ar ratios for these standards, which provide a direct comparison of the performance of the amplifiers without the effect of the ion counting multiplier used to measure ^{36}Ar, are shown in Figure 5. For the different shot sizes, the Xact amplifiers produced standard deviations of 0.43%, 3.07%, and 27.9%, respectively, while the ATONA amplifiers produced standards deviations of 0.21%, 1.35%, and 7.87%. As predicted based on zero-beam noise measurements, the ATONA outperforms the Xact for all signal sizes. The improvement between the Xact and the ATONA is greater for smaller beam sizes because the effect of amplifier ~~Johnson~~ J–N noise on the total uncertainty comes to dominate over other factors like source instability when the signal is smaller.

In order to provide a more rigorous assessment of the ATONA amplifiers themselves and to produce an amplifier-only dataset for ^{40}Ar/^{36}Ar, which is a more commonly discussed isotope ratio in ^{40}Ar/^{39}Ar geochronology, we then switched to single collector mode. Using the ATONA amplifiers, we measured each species by peak-hopping on the H2 collector, which is normally used for ^{40}Ar, and we measured ^{40}Ar/^{38}Ar and ^{40}Ar/^{36}Ar for splits of our air standard ranging from 200% (representing two

aliquots of the full standard, 1.7×10^{-12} moles of Ar, or a beam of approximately 14400 fA) to 0.36%, representing three splits with the extraction line, or approximately 3×10^{-15} moles of Ar and a beam of 25.9 fA. The $^{40}Ar/^{36}Ar$ ratios for these measurements are shown in Figure 6, and the $^{40}Ar/^{38}Ar$ ratios are shown in Figure A1. The measured ratios along with internal uncertainties and standard deviations between analyses are shown in Table 2 for $^{40}Ar/^{36}Ar$, and in Table A1 for $^{40}Ar/^{38}Ar$.

Finally, we measured the same ion beam (^{40}Ar) repeatedly on each Faraday detector to determine the gain bias between the different ATONA amplifiers. Choosing the axial detector as a reference, the relative gains of the other detectors ranged was between 1.6 and 3.6 ‰ lower, with a standard deviation of between 106 and 220 ppm for the intercalibration factor of each detector when measured using 1-second integration periods for 10 periods of 10 seconds on each detector (Figure A2). Because we used a real Ar beam measured with a sequential peak hop rather than a synthetically produced calibration voltage, fluctuations in the ion source and mass analyzer electronics might also contribute noise to these measurements, so this is a maximum estimate of the intercalibration drift of the ATONA. The production model of the ATONA amplifiers, which are now being installed on some TIMS instruments, have a calibration voltage that eliminates these other sources of uncertainty; preliminary results from this system show a standard deviation of only 0.6 ppm for each detector when measured using two-minute integration periods over multiple four hour blocks (Szymanowski and Schoene, 2019).

Because the uncertainty of the measured signals is dominated by the thermal noise of the Faraday amplifier, the uncertainty of each measured ratio is controlled largely by the uncertainty of the smaller isotope. For comparison to other instruments, we plot each measured isotope ratio as a function of the sample size of the small isotope in the ratio in Figure 7 (that is, for the same air standard, the $^{40}Ar/^{36}Ar$ ratio will plot approximately five times higher in terms of sample size than the $^{40}Ar/^{38}Ar$ ratio, because the $^{40}Ar/^{36}Ar$ ratio of air is 298.56 while the $^{40}Ar/^{38}Ar$ ratio of air is 1583.87 (Lee et al., 2006; Mark et al., 2011). This reference frame allows us to compare unlike detectors such as analog multipliers and Faraday cups, as well as to compare isotope ratios measured using a mix of detector types, such as the $^{40}Ar/^{36}Ar$ ratios measured in the standard multicollection mode of our NGX. While a better reference frame for direct comparison of detector technologies might be beam size rather than sample size, the latter choice allows for a more realistic comparison of mass spectrometers as they are used in the laboratory. We also note that while most noble gas mass spectrometers provide a similar specification for constant pressure ion source sensitivity, field reports indicate that some (notably the Thermo Argus) have an advantage due to both smaller volume and higher constant pressure sensitivity. These results show a clear improvement for the NGX with ATONA compared to the previous generation of mass spectrometer (represented by the LDEO VG 5400) and the NGX with XAct 10^{12} Ω RTIA (the same NGX at LDEO, with its original amplifiers). The performance is also better than published data for the Thermo Argus with 10^{12} Ω RTIA (Mark et al., 2009), despite the Argus' apparently higher source sensitivity, which is consistent with the prediction that the ATONA will easily outperform a 10^{12} Ω RTIA (Figure 3); see Section 3.3 for a comparison to the Argus with a 10^{13} Ω RTIA. Finally, the NGX using its ion counting multiplier in peak-hopping mode is still able to achieve a much lower noise level for very small samples, comparable to the Nu Noblesse with multiple ion counting multipliers (Jicha et al., 2016), which is also consistent with the predicted noise level of the ATONA. However, these detectors are limited to very small

samples; the data points with more than 10^{-17} moles of ^{36}Ar in Figure 7 actually use an ATONA for the ^{40}Ar beam, but we plot them in the ICM category because the uncertainty of the small isotope controls the uncertainty of the ratio measurement.

3.3 APIS cocktail standards

The Argon Intercalibration Pipette System (APIS) is a system designed to provide a portable set of argon gas standards of different size and isotope ratio for a noble gas mass spectrometer (Turrin et al., 2015). The APIS has three standard tanks containing air, a cocktail representing argon with a ^{40}Ar/^{39}Ar ratio typical of an irradiated Alder Creek sanidine standard, and a cocktail representing argon with a ^{40}Ar/^{39}Ar ratio typical of an irradiated Fish Canyon Tuff sanidine standard. Each tank has three pipettes attached to it, with volumes of 0.1, 0.2, and 0.4 cc, allowing aliquots of gas ranging in size from 1 to 7 times the size of the 0.1 cc pipette to be extracted without resorting to multiple aliquots from a single pipette. We measured each possible size, 0.1 cc, 0.2 cc, 0.3 cc, 0.4 cc, 0.5 cc, 0.6 cc, and 0.7 cc, three times from each of the Alder Creek and Fish Canyon Tuff tanks, and six times from the ~~air standard~~APIS air standard tank, interspersed with ~~our lab standard~~ the lab air standard described earlier and procedural blanks.

The APIS standards have accumulated air background since the system was first deployed, so a direct comparison of measured ratios between labs is not possible. However, we can compare air-corrected values for the Fish Canyon and Alder Creek standard tanks—similar to what would be measured during an actual experiment. As an example, we plot measured radiogenic ^{40}Ar*/^{39}Ar values (^{40}Ar/^{39}Ar ratios corrected for air contamination using simultaneously measured ^{40}Ar*/^{36}Ar ratios) for the Fish Canyon analog from the Isotopx NGX with the ATONA (10-second integration periods; 400 seconds measurement time) and the Thermo Argus with the 10^{12} Ω and 10^{13} Ω RTIA ~~(1-second integration periods; 400 seconds measurement time; Figure 8; ?)~~ (1-second integration periods; 400 seconds measurement time; Figure 8; Ross and Mcintosh, 2016)). While the ATONA exhibits lower noise on a per-signal basis, the higher sensitivity of the Argus ion source makes the results indistinguishable.

4 Summary

The ATONA amplifier represents a significant step forward in Faraday cup amplifier technology for noble gas mass spectrometry. The ATONA allows a greater dynamic range of ion beams to be measured compared to existing RTIA technology, and only highly specialized RTIA electronics are able to compete with the low noise of the ATONA. The ~~noise and gain bias of the~~ amplifiers are significantly more stable ~~than both RTIAs and~~ and have higher dynamic range than ion-counting electron multipliers. Other types of mass spectrometer that produce a stable ion beam are likely to see an even greater performance improvement with the ATONA because of its ability to capitalize on long integration times to reduce noise. The strengths of the ATONA, combining low noise for small samples with high dynamic range and good stability for large samples, are in harmony with the current priorities of the field of noble gas geochemistry, which require instruments that can deliver both high precision and flexibility for measuring a wide range of sample types.

Author contributions. SEC installed the instrument, set up hardware and software, designed experiments, performed measurements, and interpreted the results. SRH designed experiments, performed measurements, and interpreted results. DT designed and implemented the ATONA system and installed the prototype on the NGX at LDEO.

Competing interests. DT is an employee of Isotopx, Ltd.

Acknowledgements. We thank Daniel Wielandt and Trevor Ireland for thoughtful reviews that contributed to the value of the manuscript, and Klaudia Kuiper for a public comment that also contributed to the value of the manuscript. We thank Jake Ross for extensive discussion and Pychron programming help and for sharing raw data from NMGRL measurements published in conference proceedings and Brian Jicha for discussion and for sharing raw data from WiscAr mesaurements published in *Chemical Geology*. We also thank Chris Varden for initial installation and testing of the NGX at LDEO.

References

Bayer, R., Schlosser, P., Bönisch, G., Rupp, H., Zaucker, F., and Zimmek, G.: Performance and Blank Components of a Mass Spectrometric System for Routine Measurement of Helium Isotopes and Tritium by the 3He Ingrowth Method, Springer Berlin Heidelberg, Berlin, Heidelberg, https://doi.org/10.1007/978-3-642-48373-8, http://link.springer.com/10.1007/978-3-642-48373-8, 1989.

Burnard, P. G. and Farley, K. A.: Calibration of pressure-dependent sensitivity and discrimination in Nier-type noble gas ion sources: TECHNICAL BRIEF, Geochemistry, Geophysics, Geosystems, 1, n/a–n/a, https://doi.org/10.1029/2000GC000038, http://doi.wiley.com/10.1029/2000GC000038, 2000.

Coble, M. A., Grove, M., and Calvert, A. T.: Calibration of Nu-Instruments Noblesse multicollector mass spectrometers for argon isotopic measurements using a newly developed reference gas, Chemical Geology, 290, 75–87, https://doi.org/10.1016/j.chemgeo.2011.09.003, https://linkinghub.elsevier.com/retrieve/pii/S0009254111003524, 2011.

Esat, T. M.: Charge collection thermal ion mass spectrometry of thorium, International Journal of Mass Spectrometry and Ion Processes, 148, 159–170, https://doi.org/10.1016/0168-1176(95)04234-C, https://linkinghub.elsevier.com/retrieve/pii/016811769504234C, 1995.

Espanon, V. R., Honda, M., and Chivas, A. R.: Cosmogenic 3He and 21Ne surface exposure dating of young basalts from Southern Mendoza, Argentina, Quaternary Geochronology, 19, 76–86, https://doi.org/10.1016/j.quageo.2013.09.002, https://linkinghub.elsevier.com/retrieve/pii/S1871101413000769, 2014.

Ireland, T., Schram, N., Holden, P., Lanc, P., Ávila, J., Armstrong, R., Amelin, Y., Latimore, A., Corrigan, D., Clement, S., Foster, J., and Compston, W.: Charge-mode electrometer measurements of S-isotopic compositions on SHRIMP-SI, International Journal of Mass Spectrometry, 359, 26–37, https://doi.org/10.1016/j.ijms.2013.12.020, https://linkinghub.elsevier.com/retrieve/pii/S1387380613004569, 2014.

Jicha, B. R., Rhodes, J. M., Singer, B. S., and Garcia, M. O.: 40Ar/39Ar geochronology of submarine Mauna Loa volcano, Hawaii, Journal of Geophysical Research: Solid Earth, 117, https://doi.org/10.1029/2012JB009373, http://doi.wiley.com/10.1029/2012JB009373, 2012.

Jicha, B. R., Singer, B. S., and Sobol, P.: Re-evaluation of the ages of 40Ar/39Ar sanidine standards and supereruptions in the western U.S. using a Noblesse multi-collector mass spectrometer, Chemical Geology, 431, 54–66, https://doi.org/10.1016/j.chemgeo.2016.03.024, https://linkinghub.elsevier.com/retrieve/pii/S0009254116301474, 2016.

Lee, J.-Y., Marti, K., Severinghaus, J. P., Kawamura, K., Yoo, H.-S., Lee, J. B., and Kim, J. S.: A redetermination of the isotopic abundances of atmospheric Ar, Geochimica et Cosmochimica Acta, 70, 4507–4512, https://doi.org/10.1016/j.gca.2006.06.1563, https://linkinghub.elsevier.com/retrieve/pii/S0016703706018679, 2006.

Lu, Z.-T., Schlosser, P., Smethie, W., Sturchio, N., Fischer, T., Kennedy, B., Purtschert, R., Severinghaus, J., Solomon, D., Tanhua, T., and Yokochi, R.: Tracer applications of noble gas radionuclides in the geosciences, Earth-Science Reviews, 138, 196–214, https://doi.org/10.1016/j.earscirev.2013.09.002, https://linkinghub.elsevier.com/retrieve/pii/S0012825213001517, 2014.

Mark, D., Stuart, F., and de Podesta, M.: New high-precision measurements of the isotopic composition of atmospheric argon, Geochimica et Cosmochimica Acta, 75, 7494–7501, https://doi.org/10.1016/j.gca.2011.09.042, https://linkinghub.elsevier.com/retrieve/pii/S0016703711005631, 2011.

Mark, D. F., Barfod, D., Stuart, F. M., and Imlach, J.: The ARGUS multicollector noble gas mass spectrometer: Performance for 40Ar/39Ar geochronology, Geochemistry, Geophysics, Geosystems, 10, n/a–n/a, https://doi.org/10.1029/2009GC002643, http://doi.wiley.com/10.1029/2009GC002643, 2009.

Mark, D. F., Renne, P. R., Dymock, R. C., Smith, V. C., Simon, J. I., Morgan, L. E., Staff, R. A., Ellis, B. S., and Pearce, N. J.: High-precision 40Ar/39Ar dating of pleistocene tuffs and temporal anchoring of the Matuyama-Brunhes boundary, Quaternary Geochronology, 39, 1–23, https://doi.org/10.1016/j.quageo.2017.01.002, https://linkinghub.elsevier.com/retrieve/pii/S1871101417300055, 2017.

Nier, A. O.: A Mass Spectrometer for Routine Isotope Abundance Measurements, Review of Scientific Instruments, 11, 212–216, https://doi.org/10.1063/1.1751688, http://aip.scitation.org/doi/10.1063/1.1751688, 1940.

Nier, A. O.: A Mass Spectrometer for Isotope and Gas Analysis, Review of Scientific Instruments, 18, 398–411, https://doi.org/10.1063/1.1740961, http://aip.scitation.org/doi/10.1063/1.1740961, 1947.

Nyquist, H.: Thermal Agitation of Electric Charge in Conductors, Physical Review, 32, 110–113, https://doi.org/10.1103/PhysRev.32.110, https://link.aps.org/doi/10.1103/PhysRev.32.110, 1928.

Renne, P. R., Swisher, C. C., Deino, A. L., Karner, D. B., Owens, T. L., and DePaolo, D. J.: Intercalibration of standards, absolute ages and uncertainties in 40Ar/39Ar dating, Chemical Geology, 145, 117–152, https://doi.org/10.1016/S0009-2541(97)00159-9, https://linkinghub.elsevier.com/retrieve/pii/S0009254197001599, 1998.

Reynolds, J. H.: High Sensitivity Mass Spectrometer for Noble Gas Analysis, Review of Scientific Instruments, 27, 928–934, https://doi.org/10.1063/1.1715415, http://aip.scitation.org/doi/10.1063/1.1715415, 1956.

Rose, J. and Koppers, A. A.: Simplifying Age Progressions within the Cook-Austral Islands using ARGUS-VI High-Resolution ^{40} Ar/ ^{39} Ar Incremental Heating Ages, Geochemistry, Geophysics, Geosystems, 20, 4756–4778, https://doi.org/10.1029/2019GC008302, https://onlinelibrary.wiley.com/doi/abs/10.1029/2019GC008302, 2019.

Ross, J. and Mcintosh, W.: Pychron: Everything you didn't know you wanted in a geochronology application [127-13], in: Geological Society of America Abstracts with Programs, vol. 48, The Geological Society of America, Denver, CO, https://doi.org/10.1130/abs/2016AM-286732, 2016.

Sprain, C. J., Renne, P. R., Wilson, G. P., and Clemens, W. A.: High-resolution chronostratigraphy of the terrestrial Cretaceous-Paleogene transition and recovery interval in the Hell Creek region, Montana, Geological Society of America Bulletin, 127, 393–409, https://doi.org/10.1130/B31076.1, https://pubs.geoscienceworld.org/gsabulletin/article/127/3-4/393-409/126101, 2015.

Szymanowski, D. and Schoene, B.: U–Pb TIMS Geochronology Using ATONA Amplifiers [V11D-0124], in: AGU Fall Meeting 2019, AGU, San Francisco, CA, 2019.

Turrin, B. D., Swisher, III, C. C., Hemming, S. R., Renne, P. R., Deino, A. L., Hodges, K. V., Van Soest, M. C., and Heizler, M. T.: An Update to the EARTHTIME Argon Intercalibration Pipette System (APIS): Smoking from the Same Pipe, in: AGU, Fall Meeting 2015, pp. V53H–08, AGU, San Francisco, CA, https://agu.confex.com/agu/fm15/meetingapp.cgi/Paper/84132, 2015.

Wijbrans, J., Schneider, B., Kuiper, K., Calvari, S., Branca, S., De Beni, E., Norini, G., Corsaro, R. A., and Miraglia, L.: 40Ar/39Ar geochronology of Holocene basalts; examples from Stromboli, Italy, Quaternary Geochronology, 6, 223–232, https://doi.org/10.1016/j.quageo.2010.10.003, https://linkinghub.elsevier.com/retrieve/pii/S1871101410000658, 2011.

Zhang, X., Honda, M., and Hamilton, D.: Performance of the High Resolution, Multi-collector Helix MC Plus Noble Gas Mass Spectrometer at the Australian National University, Journal of The American Society for Mass Spectrometry, 27, 1937–1943, https://doi.org/10.1007/s13361-016-1480-3, http://link.springer.com/10.1007/s13361-016-1480-3, 2016.

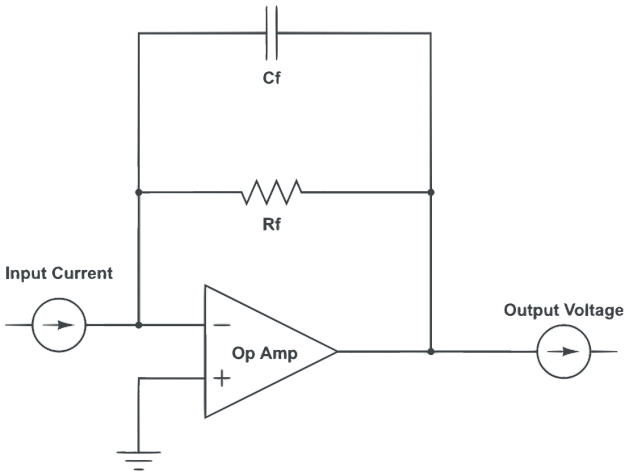

Figure 1. Schematic of a transimpedance amplifier. Note that practical examples are far more complex. The circuit consists of an op-amp, which is the active element that converts the input current to a proportional output voltage, and then a feedback resistor and capacitor that determine the gain of the circuit. In a traditional resistance transimpedance amplifier, the resistor is very high value and the capacitance is reduced as much as is practical. The ATONA instead uses a defined capacitance as the feedback element.

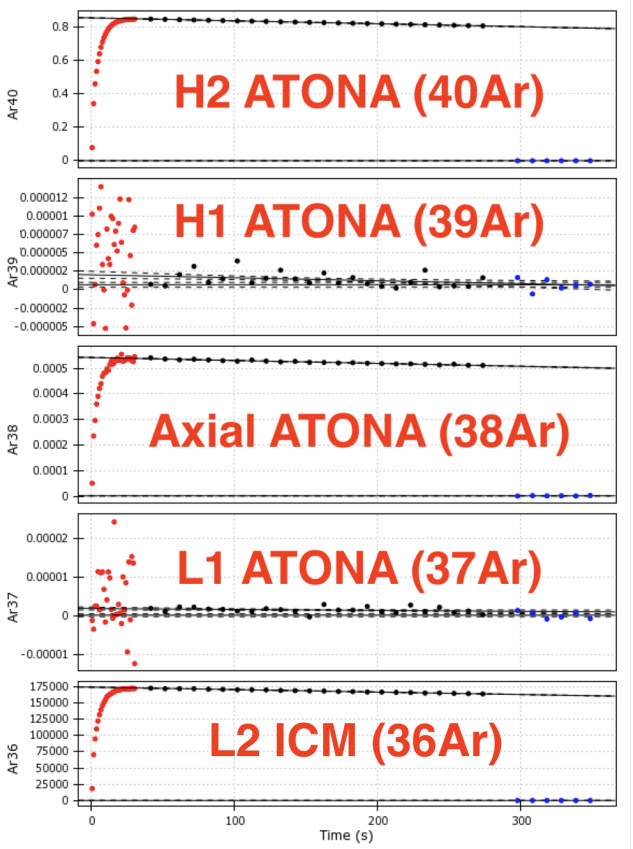

Figure 2. An example measurement of the 8.5×10^{-13} mole ^{40}Ar air standard on the Isotopx NGX. The gas is measured with a one-second integration time during 30 seconds of sample inlet, then with a ten-second integration time during 240 seconds of measurement and 60 seconds of baseline measurement. The figure shows the live measurement screen displayed in Pychron during automated sample analysis with overlain labels. Each signal is displayed as reported by the Isotopx software: volts for the four Faraday collectors (converted by the onboard ATONA firmware to equivalent 10^{11} Ω RTIA volts) and counts per second for the ion counting electron multiplier.

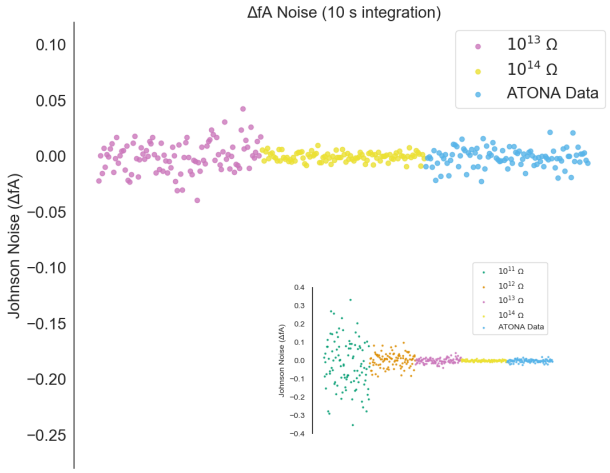

Figure 3. Measured noise on the ATONA amplifiers expressed as deviations from the average signal with no ion beam in the mass spectrometer compared to ideal 10^{13} Ω and 10^{14} Ω RTIA noise. The signals are converted to equivalent ion beam current (see Section 3.1. Each measurement and ideal RTIA calculation is made over ten seconds of integration and then simply plotted in order. The inset includes 10^{11} Ω and 10^{12} Ω examples as well, with the same ATONA data. Examples using 1-second and 100-second integration times are included in the appendix (Figures A3 and A4), as is the full version of the inset (Figure A5).

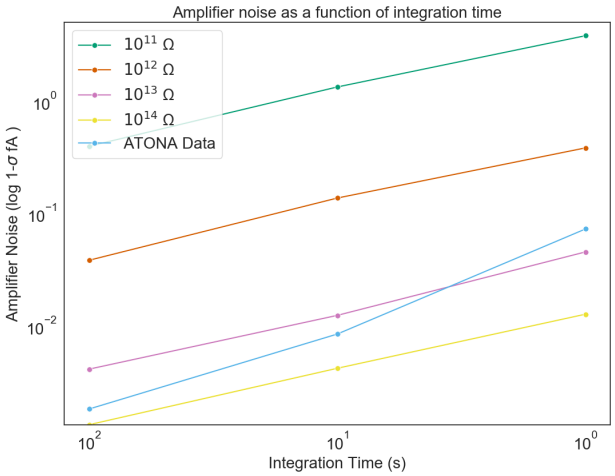

Figure 4. Noise expressed as standard deviation of signal measured (ATONA) or calculated (ideal RTIA) for the ATONA and 10^{11} Ω, 10^{12} Ω, 10^{13} Ω, and 10^{14} Ω RTIA. The ATONA noise decreases more quickly with increasing integration time because of the $1/t$ (rather than $1/\sqrt{t}$) relationship between noise and integration time.

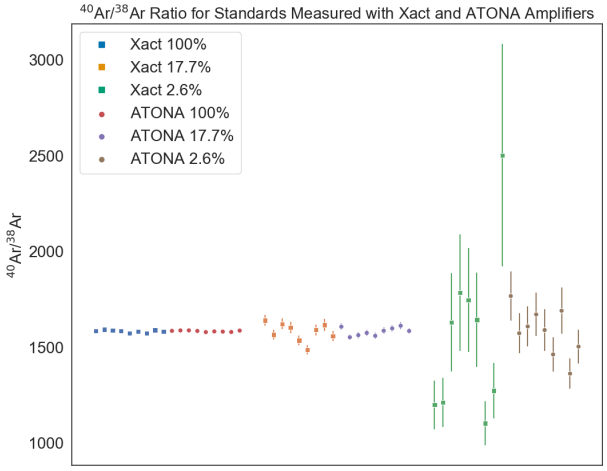

Figure 5. ^{40}Ar/^{38}Ar ratios for air standard splits of 100%, 17.7%, and 2.6% measured using both the Isotopx Xact (10^{11} Ω for ^{40}Ar and 10^{12} Ω for ^{38}Ar) amplifiers and the ATONA amplifiers in multicollection mode. Each sequence shows isotope ratios calculated from blank-corrected ratios of extrapolated peak heights for nine air standards measured sequentially, interspersed with blanks between each standard, for 600 seconds each. The ATONA measurements and the Xact measurements were both made using 600 1-second integration periods; ATONA performance improves even further with longer integration periods.

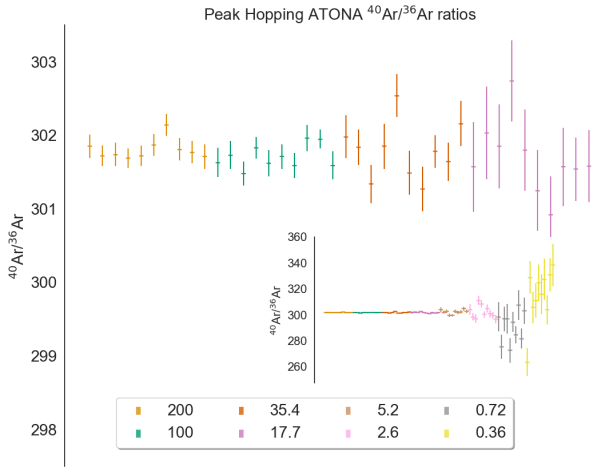

Figure 6. ^{40}Ar/^{36}Ar ratios for air standard splits ~~between~~ from 200% ~~and~~ to 17.7% (inset: 200% and 0.36%) measured using the Isotopx ATONA amplifiers in single collector peak-hopping mode, with the ^{36}Ar, ^{38}Ar, and ^{40}Ar beams measured in sequence on the H2 Faraday. Each beam was measured in sets of three 10-second integration periods, which repeated ten times. Isotope ratios are calculated from blank-corrected ratios of extrapolated peak heights. Each sequence shows ten air standards, plotted interspersed for comparison.

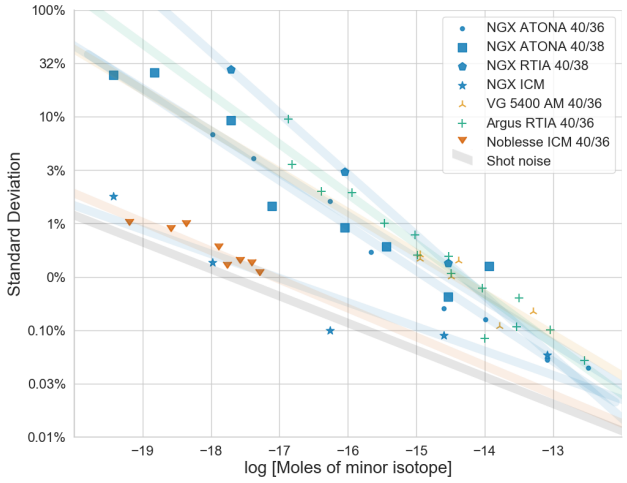

Figure 7. Standard deviation of measured ^{40}Ar/^{36}Ar or ^{40}Ar/^{38}Ar ratios for air standards measured on different mass spectrometers as a function of small isotope abundance in moles (see Section 3.2 for description of data sources). Isotope ratios are calculated from blank-corrected ratios of extrapolated peak heights. The shaded lines are linear fits to each dataset, included primarily as a visual guide. ATONA is the ATONA amplifier described here, RTIA is a traditional resistor transimpedance Faraday amplifier, ICM is an ion counting multiplier, and AM is an analog multiplier. The NGX data points with more than 10^{-17} moles of ^{36}Ar use an ATONA for the ^{40}Ar beam, but in all cases the uncertainty of the small isotope controls the uncertainty of the ratio. This plot provides a direct comparison of whole instrument performance rather than detector performance because the ion source and mass analyzer also contribute to uncertainty in the measurements, and the sample abundance is not weighted by source sensitivity. We note that we are not able to completely control for the effects of different analytical conditions, including background, detector integration time, total measurement time, sensitivity, and data reduction. The limit of shot noise, or counting noise, is shown in grey assuming no other sources of uncertainty and a regression through 600 seconds of analysis. The uncertainty of all detectors will approach this limit at large signals. Note that the uncertainty of the regression is approximately twice the uncertainty one would calculate from an average over the same interval in a mass spectrometry system without an evolving signal.

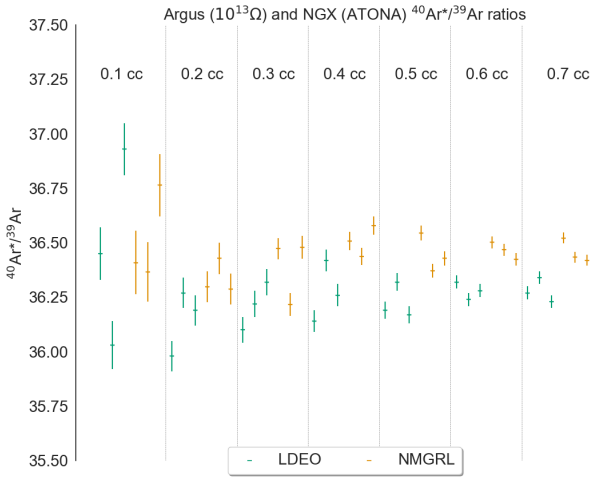

Figure 8. Air-corrected ~~^{40*} Ar~~ ^{40} Ar*/^{39}Ar ratios for the APIS Fish Canyon Tuff analog standard on the Isotopx NGX with the ATONA at Lamont-Doherty Earth Observatory and the Thermo Argus with the 10^{12} Ω and 10^{13} Ω RTIA at the New Mexico Geochronology Research Laboratory ~~(?)~~(Ross and Mcintosh, 2016), with smaller (0.1 cc) aliquots on the left, and 0.2, 0.3, 0.4, 0.5, 0.6, and 0.7 cc aliquots to the right. Both sets of measurements were performed with 400 seconds of analysis time in multicollection. Isotope ratios are calculated from blank-corrected ratios of extrapolated peak height, with the ^{40} Ar* corrected for air contaminatio using the measured ^{36} Ar. By design, the APIS experiments were conducted according to the same blank and standard protocols in each lab. The ATONA data were collected using 10-second integration periods, while the Argus data were collected using 1-second integration periods. The standard deviation of the signals for a given size aliquot is comparable for the two instruments.

Table 1. Standard deviation of the background noise (in fA) for ideal RTIAs and actual standard deviation for measurements for the ATONA with no ion beam (also in fA). A 1 fA beam would produce 0.1 mV on a 10^{11} Ω RTIA.

	10^{11} Ω RTIA	10^{12} Ω RTIA	10^{13} Ω RTIA	10^{14} Ω RTIA	ATONA
1 second	0.4065498	0.12983724	0.04049524	0.01278319	0.07310124
10 second	0.12743643	0.04051549	0.01269869	0.00408956	0.00850963
100 second	0.04053762	0.01276568	0.00407741	0.00128429	0.00183472

Appendix A: Johnson–Nyquist Noise Calculation

Thermal Johnson–Nyquist noise (J–N noise) is described by Equation 4 from Nyquist (1928):

$$V^2 = 4RK_BT, \tag{A1}$$

where V is the voltage at the frequency of interest, R is the resistance of the circuit, K_B is the Boltzmann constant, and T is the temperature. We rearrange this to solve for voltage noise and then divide by the resistance of the circuit to arrive at the noise fluctuations in terms of beam current I .

$$\sigma_I = \sqrt{4RK_BT}/R \tag{A2}$$

This equation is the basis for the calculations shown in Figures 3, 4, A3, A4, A5, A6, and A7.

Table 2. $^{40}Ar/^{36}Ar$ of air standards measured in peak-hopping mode on a single ATONA Faraday cup on the LDEO NGX. Standards were measured using ten cycles each of three ten-second integration periods for each isotope, in the order ^{36}Ar, ^{38}Ar, ^{40}Ar. Uncertainties are 1-σ standard deviation.

Split Size	200%		100%		35.4%		17.7%		5.2%		2.6%		0.72%		0.36%	
Moles	1.7E-12		8.5E-13		3.0E-13		1.5E-13		4.4E-14		2.2E-14		6.1E-15		3.1E-15	
^{36} Ar (fA)	48		25		8.6		4.2		1.2		0.60		0.18		0.081	
	$^{40}Ar/^{36}Ar$	±	$^{40}Ar/^{36}Ar$	±	$^{40}Ar/^{36}Ar$	±	$^{40}Ar/^{36}Ar$	±	$^{40}Ar/^{36}Ar$	±	$^{40}Ar/^{36}Ar$	±	$^{40}Ar/^{36}Ar$	±	$^{40}Ar/^{36}Ar$	±
	301.85	0.16	301.63	0.2	301.98	0.29	301.57	0.61	303.95	1.95	304.18	4.07	298.44	11.21	263.6	10.83
	301.72	0.14	301.73	0.19	301.84	0.24	302.03	0.63	301.91	1.17	298.3	2.88	275.24	9.29	328.75	12.51
	301.74	0.16	301.48	0.16	301.34	0.26	301.85	0.57	302.75	1.39	297.1	3.14	296.75	9.44	305.53	11.93
	301.69	0.13	301.83	0.15	301.85	0.31	302.74	0.55	299.69	1.31	310.96	3.49	296.99	11.28	311.06	13.04
	301.72	0.14	301.62	0.18	302.54	0.29	301.8	0.55	299.5	0.99	308.39	2.59	272.54	9.51	324.64	14.03
	301.87	0.15	301.71	0.17	301.49	0.3	301.25	0.55	302.6	1.32	300.24	2.4	294.46	7.82	315.81	15.25
	302.14	0.15	301.59	0.17	301.27	0.3	300.92	0.52	301.75	1.21	304.97	3.17	284.62	6.65	327.28	15.75
	301.81	0.15	301.96	0.18	301.78	0.22	301.57	0.53	302.38	1.29	300.98	3.18	307.42	11.47	303.86	11.31
	301.77	0.15	301.95	0.13	301.64	0.26	301.54	0.43	304.76	1.52	299.41	2.62	281.71	7.78	330.93	12.68
	301.71	0.17	301.59	0.19	302.16	0.31	301.58	0.49	302.64	1.41	296.59	3.09	303.07	9.99	338.41	16.31
Average	301.8		301.7		301.8		301.7		302.2		302		291		315	
SD (1-σ)	0.13		0.16		0.38		0.48		1.6		4.9		12		21	
SD (1-σ (%)	0.044%		0.053%		0.13%		0.16%		0.54%		1.6%		4.1%		6.8%	

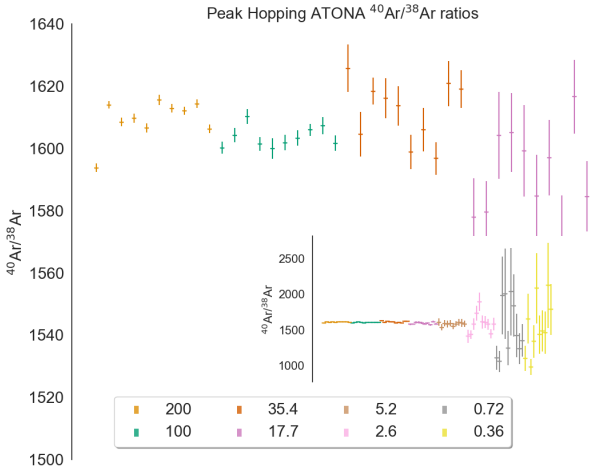

Figure A1. $^{40}Ar/^{38}Ar$ ratios for air standard splits ~~between~~ from 200% ~~and~~ to 17.7% (inset: 200% and 0.36%) measured using the Isotopx ATONA amplifiers in single collector peak-hopping mode, with the ^{36}Ar, ^{38}Ar, and ^{40}Ar beams measured in sequence on the H2 Faraday. Each beam was measured in sets of three 10-second integration periods, which repeated ten times. Each sequence shows ten air standards, plotted interspersed for comparison.

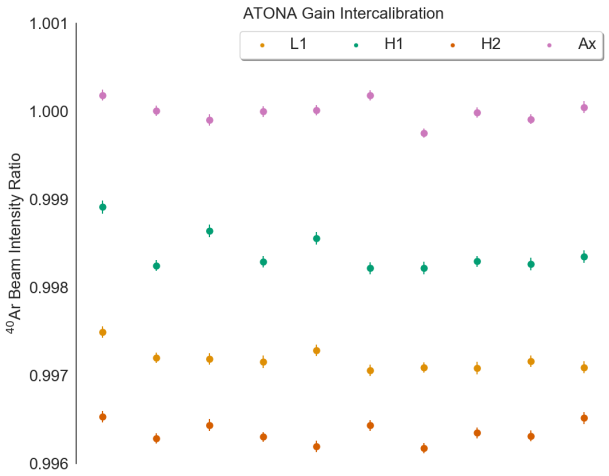

Figure A2. Intercalibration measurements using an ^{40}Ar beam produced by aliquots of the 8.5×10^{-13} mole air standard, measured by peak hopping just the ^{40}Ar beam on each of the four ATONA Faraday collectors on the NGX. Plotted are the ratios of each measurement of the ^{40}Ar signal on a given detector to the average of all measurements on the Axial detector. Measurements were made using sets of ten 1-second integration periods, repeated ten times sequentially on each detector, with the intensities calculated using a linear extrapolation to time-zero; internal uncertainties shown are the $1-\sigma$ standard error of the linear fit. No blank correction was made. The detector intercalibration factor ranges from 0.9964 to 0.9984 for the other three detectors relative to the axial detector, with standard deviations ranging from 106 to 220 ppm for each.

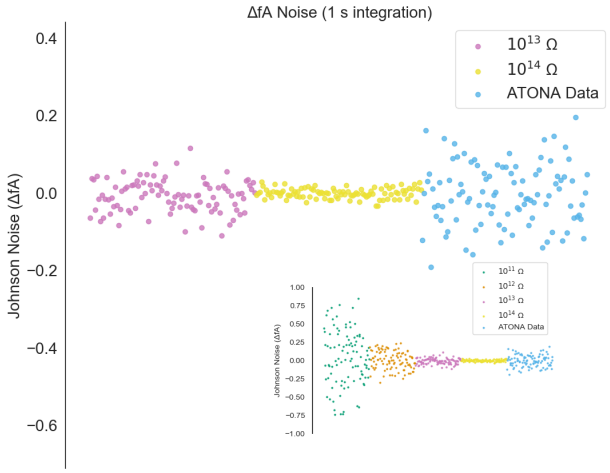

Figure A3. Measured noise on the ATONA amplifiers expressed as deviations from the average signal with no ion beam in the mass spectrometer compared to ideal 10^{13} Ω and 10^{14} Ω RTIA noise. The signals are converted to equivalent ion beam current (see Section 3.1. Each measurement and ideal RTIA calculation is made over one second of integration and then simply plotted in order. The inset includes 10^{11} Ω and 10^{12} Ω examples as well, with the same ATONA data. Examples using a 10-second integration times are included in Figure 3. The full version of the inset is provided in Figure A6

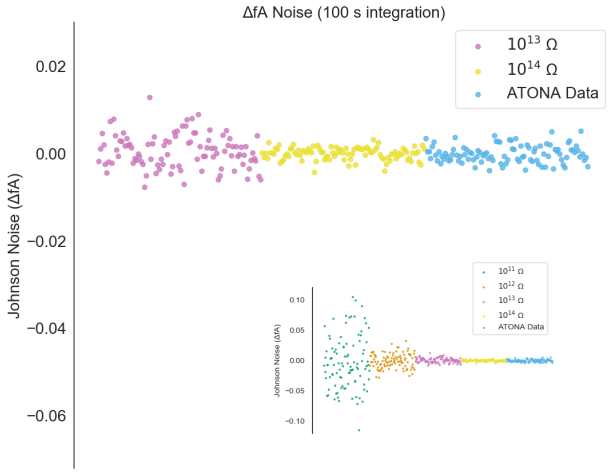

Figure A4. Measured noise on the ATONA amplifiers expressed as deviations from the average signal with no ion beam in the mass spectrometer compared to ideal 10^{13} Ω and 10^{14} Ω RTIA noise. The signals are converted to equivalent ion beam current (see Section 3.1. Each measurement and ideal RTIA calculation is made over 100 seconds of integration and then simply plotted in order. The inset includes 10^{11} Ω and 10^{12} Ω examples as well, with the same ATONA data. Examples using a 10-second integration times are included in Figure 3. The full version of the inset is provided in Figure A7

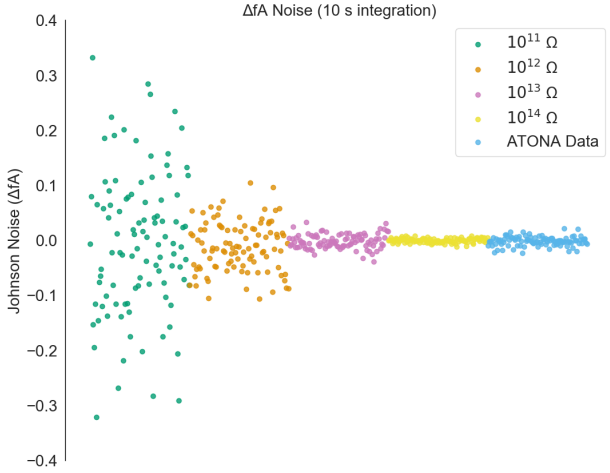

Figure A5. Measured noise on the ATONA amplifiers expressed as deviations from the average signal with no ion beam in the mass spectrometer compared to ideal 10^{11} Ω , 10^{12} Ω , 10^{13} Ω , and 10^{14} Ω RTIA noise. The signals are converted to equivalent ion beam current (see Section 3.1. Each measurement and ideal RTIA calculation is made over 10 seconds of integration and then simply plotted in order. This is the full version of the inset from Figure 3.

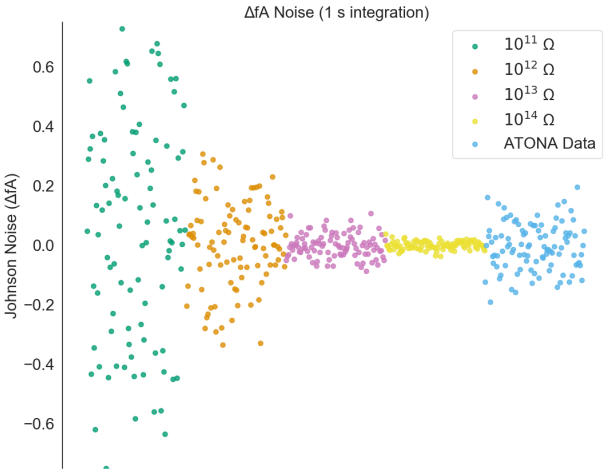

Figure A6. Measured noise on the ATONA amplifiers expressed as deviations from the average signal with no ion beam in the mass spectrometer compared to ideal 10^{11} Ω , 10^{12} Ω , 10^{13} Ω , and 10^{14} Ω RTIA noise. The signals are converted to equivalent ion beam current (see Section 3.1. Each measurement and ideal RTIA calculation is made over 10 seconds of integration and then simply plotted in order. This is the full version of the inset from Figure A3.

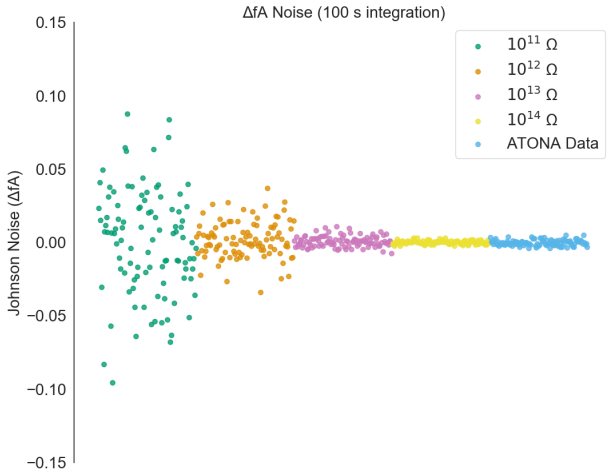

Figure A7. Measured noise on the ATONA amplifiers expressed as deviations from the average signal with no ion beam in the mass spectrometer compared to ideal 10^{11} Ω , 10^{12} Ω , 10^{13} Ω , and 10^{14} Ω RTIA noise. The signals are converted to equivalent ion beam current (see Section 3.1. Each measurement and ideal RTIA calculation is made over 10 seconds of integration and then simply plotted in order. This is the full version of the inset from Figure A4.

Table A1. $^{40}Ar/^{38}Ar$ of air standards measured in peak-hopping mode on a single ATONA Farday cup. Standards were measured using ten cycles each of three ten-second integration periods for each isotope, in the order ^{36} Ar, ^{38} Ar, ^{40} Ar. Uncertainties are 1-σ standard deviation.

Split Size	200%		100%		35.4%		17.7%		5.2%		2.6%		0.72%		0.36%	
Moles	1.7E-12		8.5E-13		3.0E-13		1.5E-13		4.4E-14		2.2E-14		6.1E-15		3.1E-15	
^{38} Ar (fA)	9.0		4.4		1.6		0.79		0.24		0.12		0.037		0.018	
	$^{40}Ar/^{38}Ar$	±	$^{40}Ar/^{38}Ar$	±	$^{40}Ar/^{38}Ar$	±	$^{40}Ar/^{38}Ar$	±	$^{40}Ar/^{38}Ar$	±	$^{40}Ar/^{38}Ar$	±	$^{40}Ar/^{38}Ar$	±	$^{40}Ar/^{38}Ar$	±
	1593.77	1.34	1600.24	1.96	1625.76	7.67	1577.95	12.48	1606.37	51.64	1410.08	91.6	1105.81	167.86	1097.03	175.99
	1614	1.23	1604.26	2.29	1604.56	7.16	1579.56	9.93	1533.66	43.81	1432.79	60.02	1055.65	147.96	1656.38	348.27
	1608.49	1.33	1610.22	2.43	1618.39	4.32	1604.27	13.97	1592.27	42.28	1581.09	77.27	1982.04	543.76	977.93	114.47
	1609.75	1.42	1601.48	2.18	1616.19	6.44	1605.08	12.7	1579.97	50.73	1732.52	102.8	2006.36	637.14	1337.71	230.81
	1606.59	1.49	1599.95	3.34	1613.67	6.25	1599.19	14.71	1591.78	45.32	1897.26	127.61	1243.5	238.71	2084	494.11
	1615.55	1.67	1601.88	2.42	1598.89	5.47	1584.81	13.06	1552.6	42.78	1610.14	89.48	2035.09	613.68	1435.19	267.91
	1612.93	1.37	1603.37	2.53	1606.04	7.01	1597.03	12.13	1585.02	39.16	1608.49	86.12	1841.06	439.03	1485.93	290.36
	1612.13	1.34	1605.97	1.92	1596.85	5.24	1570.72	14.27	1605.16	44.37	1580.82	76.43	1420.77	301.82	1462.66	298.32
	1614.38	1.33	1607.31	2.79	1620.84	7.21	1616.69	11.86	1597.96	55.59	1442.38	63.65	1236.64	214.53	2123.91	600.62
	1606.3	1.35	1601.69	2.44	1619.13	6.02	1584.63	11.23	1583.43	42.14	1580.97	91.15	1352.15	232.3	1787.73	358.78
Average	1609		1604		1612		1592		1583		1588		1528		1545	
SD (1-σ)	6.4		3.3		9.8		15		23		147		394		378	
SD (1-σ (%)	0.40%		0.21%		0.61%		0.92%		1.5%		9.3%		26%		24%	